The 2015 World Congress on
Aeronautics, Nano, Bio, Robotics, and Energy (ANBRE15)
Incheon, Korea, August 25-28, 2015

Design and Energy Modelling of a Solar Driven Combined Power-Refrigeration System with Super-Trans-Sub Critical Cycles using CO_2

*Onder Kizilkan[1)] and Ahmet Kabul[2)]

[1), 2)] *Süleyman Demirel University, Faculty of Technology, Department of Energy Systems Engineering, 32260, Isparta, Turkey*
[1)] onderkizilkan@sdu.edu.tr

ABSTRACT

In this study, a solar driven combined power-refrigeration system is designed and analyzed energetically. The combined system consists of three subsystems, a supercritical Brayton Cycle (BC), a transcritical Organic Rankine Cycle (ORC) and a subcritical Vapor Compression Refrigeration Cycle (VCRC). In all cycles, CO_2, a sustainable working fluid with no ozone depleting potential and with negligible global warming potential is used. The heat demand of the BC is supplied from solar energy by means of parabolic trough solar collectors where the rejected heat from the cycle is used for heat energy demand of Organic Rankine Cycle and the compressor of refrigeration cycle is driven by the power generated from the ORC turbine From the results, the efficiencies of BC and ORC is found to 12.9 % and 4.47 % respectively while the COP value of VCRC is determined to be 3.35. Additionally, a parametric study is carried out to determine the variation of energy efficiency rates of the three systems with the selected parameters.

1. INTRODUCTION

Since the electrical energy demands are globally increasing and the environmental concerns are preventing its matching with supply, the engineering community is being posed challenges to look for alternative ways of bridging the gap. A big number of fractions of that demand are met from traditional water based power plants either from hydroelectric or thermal energy derived from fossil fuels or nuclear reactors. Environmental emotions are preventing addition of capacities to either of those categories of power plants (Garg et al. 2013).

According to the REPRISK report on environmental, social and governance issues in the emerging markets of MINT (Mexico, Indonesia, Nigeria and Turkey), Turkey is projected to grow rapidly (Reprisk 2015), however it already has difficulties in meeting energy demand as the endogenous fossil energy resources are insufficient. In 2010, it was reported that the primary energy consumption of Turkey was more than three times higher than the country's generation capacity. This has led to Turkey's

---

[1)] Associate Professor
[2)] Associate Professor

dependency on energy imports from other countries so that nearly 70% of the national demand is being met by imported fossil fuels and their share continues to increase each year. On the other hand, Turkey has got a large potential of renewable energy resources, with leading potential of solar energy (Energy 2011, Energy 2012, Atilgan and Azapagic 2014).

Solar energy potential of Turkey is considerably high and profitable due to its geographical position in the northern hemisphere (Şenol 2012; Koca et al. 2011; Aras et al. 2006; Gunes 2001; Ulgen and Hepbasli 2004). According to the latest reported data provided by the General Directorate of Renewable Energy (sub-organization of Ministry of Energy and Natural Resources of Turkey) Turkey has an average annual total global solar radiation of 1527.46 kWh/m^2-year and annual total sunshine duration of 2741.07 h/year as seen from Fig. 1 (EIE 2014). The Ministry of Energy and Natural Resources of the Turkey has listed concentrating solar power systems as important research issues in the 'Summary of National mid & long-Term Science and Energy Technology Development Plan' (2006–2020). On the other hand, up to now, no commercial solar thermal power plant is in operation in Turkey. These technologies can easily be adapted to the most parts of Turkey due to the abundant solar radiation and the large wasteland (Kaygusuz 2011).

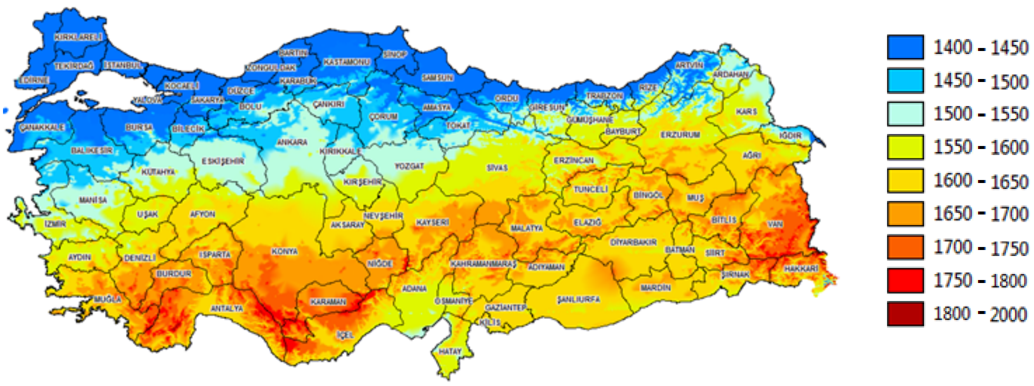

Fig. 1 Annual total solar radiation map of Turkey (kWh/m^{2}day) (EIE 2014)

Parabolic trough solar collector (PTSC) technology is considered the most established solar thermal technology for power production. This technology which is the most matured one for the large scale utilization of solar energy with high dispatchability, has been used in large power plants since the 1980s and shows a promising future (Al-Sulaiman 2013; Reddy et al. 2015).

Due to global environmental concerns, the usage of natural working fluid is becoming more interesting theme to be discussed. Carbon dioxide (CO_2) has been widely investigated to be utilized as a working fluid in refrigeration and power systems due to it has no ozone depleting potential (ODP=0) and negligible global warming potential (GWP =1). It is also inexpensive, non-explosive, non-flammable and abundant in nature. At the same time, CO_2 has advantages in use as a working fluid in low-grade heat resource recovery and energy conversion from waste heat (Garg et al. 2015). The supercritical, transcritical and subcritical CO_2 cycles are also being considered for power generation and refrigeration systems as a promising avenue with higher efficiency and cleaner solution (Iverson et al. 2013). The critical temperature (30.98 °C) and critical pressure (7377 kPa) indicate whether the cycle runs as supercritical, transcritical or subcritical cycle, the possibility for condensing and the system working pressure respectively (Garg et al. 2013).

In this study a solar driven combined power-refrigeration system working with CO_2 is modelled and analyzed to be an energy generation option for Turkey's increasing energy demand. The system includes three sub cycles: supercritical Brayton Cycle (BC), transcritical Organic Rankine Cycle (ORC) and subcritical Vapor Compression Refrigeration Cycle (VCRC). The heat energy demand of the system is supplied from solar energy by means of PTSCs. In order to evaluate the designed system performance, thermodynamic analyses of three sub-processes are carried out. With these analyses, it is aimed to encourage the use of solar energy in power generation applications and suggest modifications to the system design and operation to provide sustainable energy production.

2. SOLAR DRIVEN COMBINED POWER-REFRIGERATION SYSTEM

The investigated system consists of PTSCs, supercritical BC and transcritical ORC for power generation and subcritical VCRC for refrigeration. Since the use of CO_2 as a working-fluid of power and refrigeration cycles has been growing in recent years due to associated benefits (Singh et al. 2013), it has been selected as working fluid for all cycles. The P-h diagram of the three options which are investigated are given in Fig. 2. As seen from the figure, the top cycle is supercritical BC, in which the CO_2 operates above critical point with all gaseous phase operation. The middle cycle is transcritical ORC with condensing process below critical point and heating process above critical point. The bottom cycle is subcritical VCRC and the condensation and the evaporation processes are below the critical but condensation takes place close to the critical point.

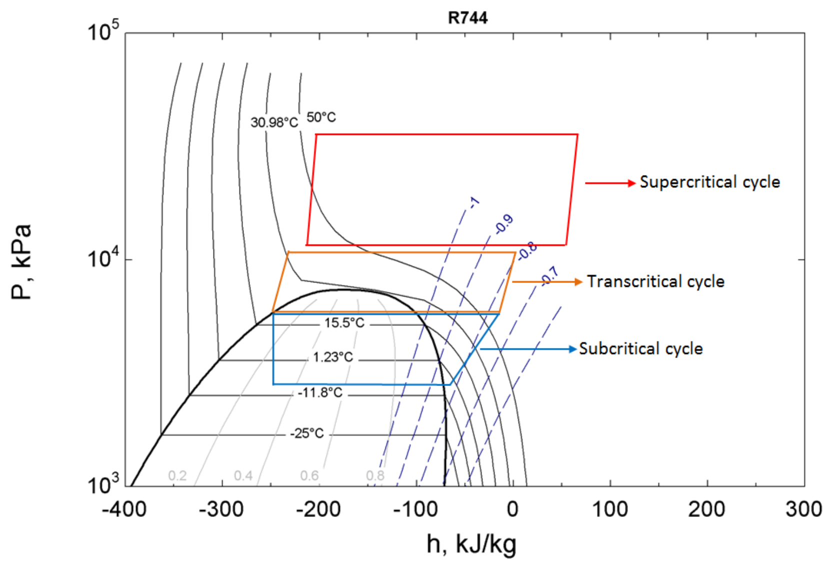

Fig. 2 The P-h diagram of the three cycles

The schematic representation of solar driven combined power-refrigeration system is shown in Fig. 3. Solar energy is collected using a PTSC system for supplying heat demand of the cycles. For PTSC system, Therminol-VP1 is selected as the heat transfer fluid (HTF) for its good heat transfer properties and good temperature control (Therminol 2014). Because of its good properties, it is being used in many high temperature applications driven by PTSC such as power plants (Kumar and Reddy 2009; Vogel et al. 2014; Cheng et al. 2012; Al-Sulaiman 2013; 2014).

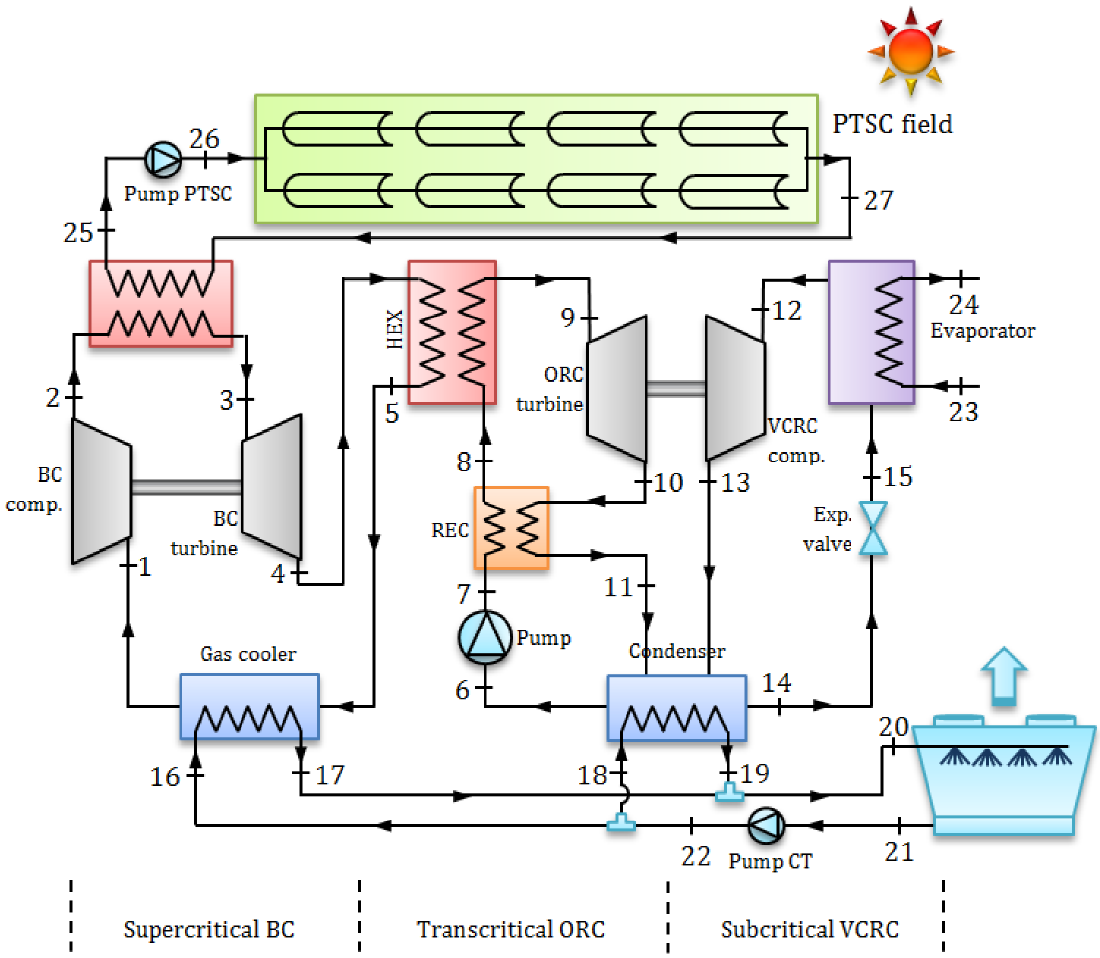

Fig. 3 Schematic representation of proposed system

In the BC, a compressor is used to increase the pressure of the gas and after compression process; the compressed gas enters to the boiler. In the boiler the gas is heated up to about 350 °C by means of the absorbed solar energy using HTF. The high pressure CO_2 then expands in the turbine and enters to the heat exchanger (HEX) where it gives the rest of its heat energy to the transcritical ORC. In gas cooler, the gas is cooled to 32 °C before the inlet of the compressor.

The ORC comprises of four compounds: a turbine, an evaporator, a condenser and a pump. The required heat energy for the evaporator of the ORC is supplied from the

BC. The liquid CO_2 from the condenser is pumped by means of liquid pump and fed to the HEX, where it is heated by the heat energy delivered from BC, and becomes superheated vapor. The superheated vapor then enters to the turbine and expands to a low pressure. At the exit of the ORC turbine, the CO_2 vapor enters to recuperator for preheating of the other fluid after pumping process. Subsequently, the turbine exhaust is intensified to liquid in the condenser by extracting heat to the environment by mans of a cooling tower.

Table 1 General design parameters of the combined system

PTSC	Pipe receiver inner diameter	0.08 m
	Pipe receiver outer diameter	0.09 m
	Glass cover diameter	0.15 m
	Total length of PTSC	2020.78 m
	Mass flow rate of HTF	25.34 kg/s
	Receiver emissivity	0.92
	Glass cover emissivity	0.87
	Temperature of the sun	5739 K
	Absorbed solar radiation	850 W/m^2
	Wind velocity	5 m/s
BC	Turbine isentropic efficiency	0.93
	Pump isentropic efficiency	0.92
	Turbine inlet temperature	350 °C
	Compressor inlet temperature	32 °C
	Turbine inlet pressure	20000 kPa
	Turbine outlet pressure	8000 kPa
	Net power generation	120 kW
ORC	Turbine isentropic efficiency	0.88
	Pump isentropic efficiency	0.96
	Turbine inlet temperature	85 °C
	Condenser temperature	28 °C
	Turbine inlet pressure	8000 kPa
	Turbine outlet pressure	6892 kPa
	Net power generation	120 kW
VCRC	Evaporator capacity	402.8 kW
	Evaporator temperature	-10 °C
	Condenser temperature	40 °C
	Entering EG-water temperature	-4 °C
	Exiting EG-water temperature	-9 °C

The ORC and the VCRC are coupled together by the turbine-compressor unit. They also use the same condenser and CO_2 as working fluid. The compressor of the VCRC is driven by the turbine of ORC system and the CO_2 is compressed to the condenser as superheated vapor. The VCRC is subcritical cycle and after the condenser, the refrigerant enters to the expansion valve where it becomes wet vapor at low pressure. After expansion valve, the refrigerant passes through evaporator where it absorbs necessary heat energy to become saturated vapor while it refrigerates the cold room.

For the refrigeration processes, the coolant is 23 % ethylene glycol – water (EG-water) mixture with a freezing temperature of -9.69 °C. Also water is used in the cooling tower for absorbing heat energy from gas cooler and condenser. The general design parameters for modelling of the power-refrigeration system are given in Tab. 1. It must be noted that data for PTSC system is adapted from the reported data in the references Soteris (2009), Singh et al (2013) and Al-Sulaiman (2014).

3. GOVERNING THERMODYNAMIC EQUATIONS

The performance of the solar driven combined power-refrigeration system is mathematically modelled using mass and energy balance equations. In order to carry out the thermodynamic analysis of the system, the assumptions below are made:

- All the operations are in steady state and steady flow processes.
- The changes in kinetic and potential energies are ignored.
- The working fluid at the inlet of ORC is assumed to be saturated liquid.
- The working fluid at the exit of evaporator of VCRC assumed to be saturated vapor.
- The turbine and pumps operations are assumed to be adiabatic.

The general mass balance equation can be written as (Cengel and Boles 2006):

$$\sum \dot{m}_{in} = \sum \dot{m}_{out} \tag{1}$$

where m is the mass flow rate and the subscripts in and out stand for entering and exiting streams to and from the system, respectively. The general energy balance can be written as:

$$\sum \dot{E}_{in} = \sum \dot{E}_{out} \tag{2}$$

where E_{in} is the ratio of net energy input to the system, E_{out} is the net energy output from the system. For steady-state, steady-flow process, the general energy balance can be also defined as:

$$\dot{Q} + \sum \dot{m}_{in} h_{in} = \dot{W} + \sum \dot{m}_{out} h_{out} \tag{3}$$

In Eq. (3), Q is the ratio of heat, W is the ratio of net work, and h is the specific enthalpy.

For the thermodynamic modelling of the PTSC system, the mathematical formulation given in reference Kalogirou (2009) is used. One can easily find some similar models for PTSC systems in some other literature (Duffie and Beckman 2013;

Tiwari 2003). The useful energy absorbed by the solar collector is defined as (Kalogirou 2009):

$$\dot{Q}_u = F_R[SA - A_r U_L (T_i - T_a)] \tag{4}$$

where F_R is the heat removal factor, S is the solar radiation intensity, A is the aperture area, A_r is the receiver area, and U_L is the solar collector overall heat loss coefficient. In Eq. (4), T stands for temperature while subscripts i and a denote inlet and ambient conditions respectively. The useful heat energy can be written as in terms of working fluid's heat capacity:

$$\dot{Q}_u = \dot{m} c_p (T_0 - T_i) \tag{5}$$

In Eq. (4), the heat removal factor F_R can be calculated from the equation below (Kalogirou 2009):

$$F_R = \frac{\dot{m} c_p}{A_r U_L}\left[1 - exp\left(\frac{-A_r U_L F'}{\dot{m} c_p}\right)\right] \tag{6}$$

where F' is the collector efficiency factor and given below:

$$F' = \frac{U_0}{U_L} \tag{7}$$

Here, U_L is the heat loss coefficient and U_0 is the overall heat transfer coefficient of the receiver of PTSC. The overall collector heat loss coefficient U_L, based on the receiver area A_r and glass cover area A_g, is written as (Kalogirou 2009):

$$U_L = \left[\frac{A_r}{(h_{c,c-a} + h_{r,c-a})A_g} + \frac{1}{h_{r,r-c}}\right]^{-1} \tag{8}$$

In Eq. (8), $h_{c,c-a}$ is the convection heat loss coefficient, between ambient and the cover, $h_{r,c-a}$ is the radiation heat transfer coefficient for the glass cover to the ambient and $h_{r,r-c}$ is the radiation heat transfer coefficient between the receiver tube and the glass cover. The equations of the mentioned coefficients are given below:

$$h_{c,c-a} = \frac{Nu_{air} k_{air}}{D_g} \tag{9}$$

$$h_{r,c-a} = \varepsilon_g \sigma (T_g + T_a)(T_g^2 + T_a^2) \tag{10}$$

$$h_{r,r-c} = \frac{\sigma (T_r + T_g)(T_r^2 + T_g^2)}{\frac{1}{\varepsilon_r} + \frac{A_r}{A_g}\left(\frac{1}{\varepsilon_g} - 1\right)} \tag{11}$$

In above equations, k is the thermal conductivity, Nu is the Nusselt number, Re is the Reynolds number, σ is Stefan–Boltzmann constant, ε is the emittance constant, subscripts r and g represent receiver and glass cover, respectively. The overall heat transfer coefficient of the receiver tube is given by:

$$U_0 = \left[\frac{1}{U_L} + \frac{D_0}{h_{fi} D_{fl}} + \left(\frac{D_0 \, ln\left(\frac{D_0}{D_i}\right)}{2k} \right) \right]^{-1} \tag{12}$$

where D_i and D_o are the inside and the outside tube diameters, h_{fi} is the heat transfer coefficient inside the tube, and k is the thermal conductivity of the tube. The heat transfer coefficient inside the tube (h_{fi}) can be calculated using Eq. (9) by adapting the equation from air to fluid. In order to determine the performances of the considered three systems, the energy efficiencies are given blow:

$$\eta_{BC} = \frac{\dot{W}_{Net,BC}}{\dot{Q}_{Boiler}} \tag{13}$$

$$\eta_{ORC} = \frac{\dot{W}_{Net,ORC}}{\dot{Q}_{HEX}} \tag{14}$$

$$COP_{VCRC} = \frac{\dot{Q}_E}{\dot{W}_{Comp}} \tag{15}$$

4. RESULTS AND DISCUSSION

The solar driven combined power-refrigeration system was analyzed based on the model and assumptions described previously. Using the general mass and energy balance equations, the analyses were made for the baseline conditions first using Engineering Equation Solver (EES) Software (F-Chart 2015). The calculated properties of the proposed combined system are given in Table 2, according to reference points represented in Fig. 2. During the calculations, the net power generation of BC was taken as 865 kW, the net power generation of ORC was taken as 120 kW and the refrigeration capacity of VCRC was taken as 402.8 kW. According to the analyses, the efficiency of BC was found to be 12.9 % while the efficiency of ORC was found to be 4.47 % and COP value of VCRC was calculated to be 3.35.

Some parametric studies were also done to see the system performance by varying the effective system parameters. For these analyses, the variable parameters were selected to be solar radiation intensity, turbine and compressor inlet pressure and temperature for BC, turbine inlet pressure and temperature for ORC, evaporator and condenser temperatures for VCRC.

Table 2 Calculated property data for the solar driven combined system

Reference point	Fluid type	T (°C)	P (kPa)	$\dot{m}$ (kg/s)	h (kJ/kg)	s (kJ/kgK)	$\dot{E}$ (kW)
1	CO_2	32	8000	12.34	-210.4	-1.426	-2596.34
2	CO_2	56.09	20000	12.34	-192	-1.422	-2369.28
3	CO_2	347.3	20000	12.34	279.1	-0.3455	3444.094
4	CO_2	251	8000	12.34	190.6	-0.3327	2352.004
5	CO_2	72.51	8000	12.34	-26.74	-0.8448	-329.972
6	CO_2	28	6892	18.01	-217.2	-1.443	-3911.77
7	CO_2	31.27	8000	18.01	-215.4	-1.443	-3879.35
8	CO_2	34.93	8000	18.01	-156.6	-1.251	-2820.37
9	CO_2	85	8000	18.01	-7.705	-0.7907	-138.767
10	CO_2	72.98	6892	18.01	-14.37	-0.7881	-258.804
11	CO_2	39.62	6892	18.01	-73.19	-0.9676	-1318.15
12	CO_2	-10	2649	2.768	-71.64	-0.8405	-198.3
13	CO_2	63.57	6892	2.768	-28.29	-0.8289	-78.3067
14	CO_2	28	6892	2.768	-217.2	-1.443	-601.21
15	CO_2	-10	2649	2.768	-217.2	-1.393	-601.21
16	Water	17.84	101.3	37.19	74.87	0.2652	2784.415
17	Water	32.4	101.3	37.19	135.8	0.4695	5050.402
18	Water	17.84	101.3	45.45	74.87	0.2652	3402.842
19	Water	34.22	101.3	45.45	143.4	0.4944	6517.53
20	Water	33.4	101.3	82.64	140	0.4832	11569.6
21	Water	17.79	101.3	82.64	74.66	0.2645	6169.902
22	Water	17.84	101.3	82.64	74.87	0.2652	6187.257
23	EG-water	-4	101.3	21.26	-41.47	-0.151	-881.652
24	EG-water	-9	101.3	21.26	-60.42	-0.222	-1284.53
25	Therminol-VP1	289.8	205.8	25.34	531.2	1.271	13460.61
26	Therminol-VP1	290	205.8	25.34	531.8	1.272	13475.81
27	Therminol-VP1	384.4	389	25.34	760.6	1.646	19273.6

Figure 4 shows the variation of solar radiation intensity with BC turbine net power generation and energy efficiency of BC respectively. As seen from the figure, turbine power generation and efficiency values are increasing by varying the solar radiation between 0.5 and 0.95 kW/m^2. Also it must be noted that the arrow in Figure 4 shows the lower limit of the solar radiation for starting up the ORC system since its working conditions depend on the heat rejected from the BC and below this range, the temperature of the CO_2 at the exit of the BC turbine is lower than the desired value. Additionally, as seen from the figure, the energy efficiency rate increases with the increase of solar radiation but the rise of energy efficiency is ranged from 12.74 % to 14.9 %. This increment can found to be a bit lower since with the increase of the solar radiation, the useful heat energy supplied by PTSC to the boiler of BC also increases.

As the energy efficiency is defined as the ratio of consumed energy to produced energy, the change of energy efficiency with solar radiation remains so less.

Figure 5 shows the variation of solar radiation intensity with turbine inlet temperature of the BC. As seen from the figure, inlet temperature of turbine increases with the increase of solar radiation. This is due to the absorbed heat energy is increased with the increment of the solar radiation which results a temperature increase at the exit of PTSC.

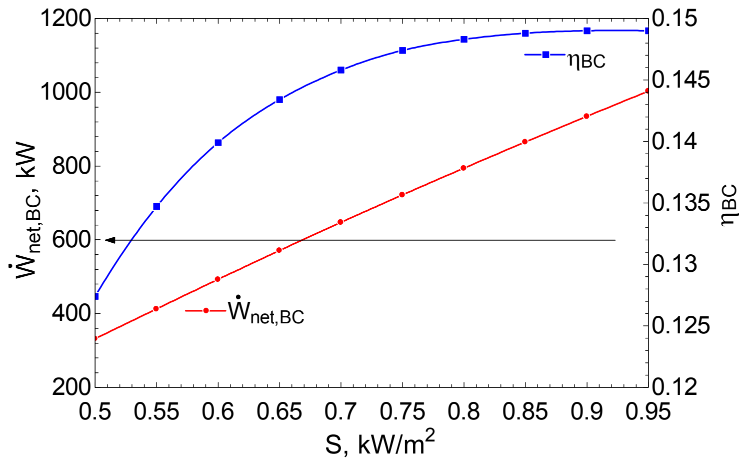

Fig. 4 Variation of solar radiation intensity with net power generation of BC and efficiency

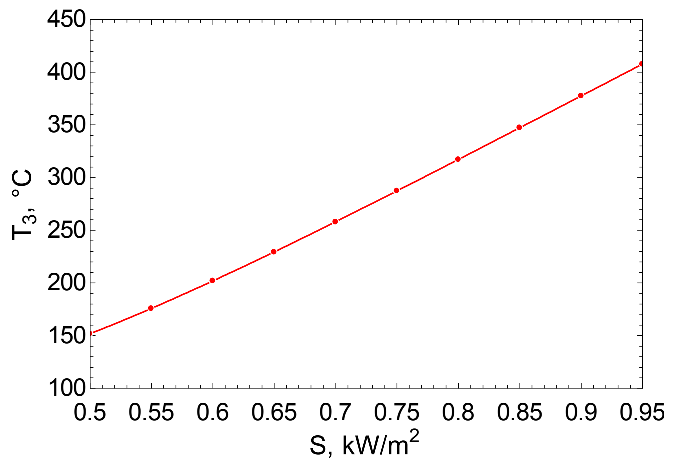

Fig. 5 Variation of solar radiation intensity with turbine inlet temperature of BC

The change of the total useful heat energy absorbed by PTSC with the change of the total aperture area is presented in Figure 6. The figure shows that with the increase of the total aperture area of the PTSC, the absorbed heat energy increases from 4384 kW to 9626 kW. The required PTSC length for the area calculated in the figure ranges between 1500 –3500 m. Also the right hand side of the y-axis shows the change of net electrical power generation of the BC with PTSC aperture area. While the area increases, the net power generation increases since the useful heat increases. The analyses here are made for only BC since the PTSC system mainly supports the boiler of BC while the other cycles are powered by the energy rejected from this cycle.

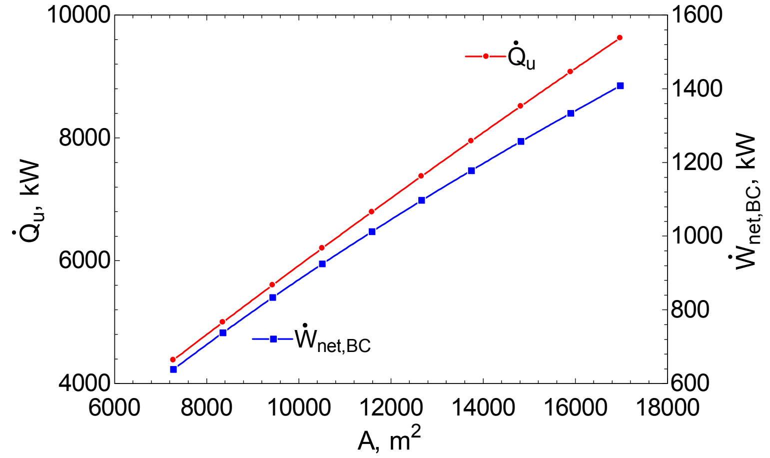

Fig. 6 Variation of aperture area of PTSC with useful heat energy and net power generation of BC

The effects of pressures and temperatures on the three considered systems were also analyzed individually in order to determine the effects on the energy efficiencies. Figure 7 shows the variation of energy efficiency with turbine inlet pressure and temperature of the BC. While the turbine inlet pressure increases, the efficiency of BC increases from 12.41 % to 16.97 % while the effect of the turbine inlet temperature on efficiency is too low. As seen from the figure, the increase of turbine inlet temperature from 300 to 380 °C, increases the BC efficiency only 0.2 %.

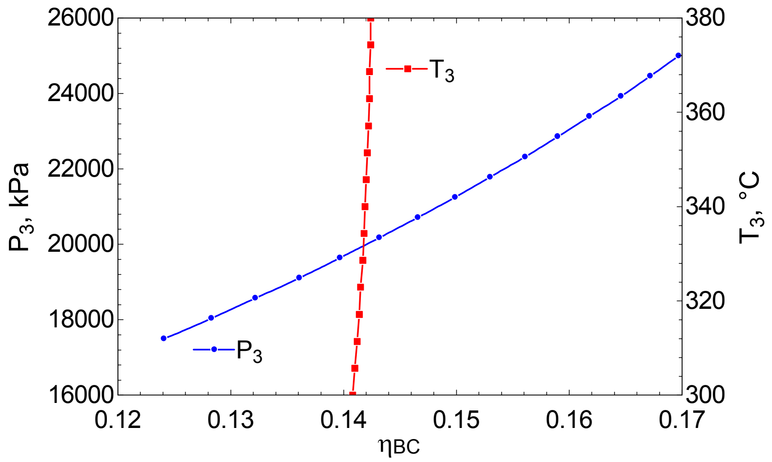

Fig. 7 Variation of energy efficiency with turbine inlet pressure and temperature of BC

The effects of compressor inlet pressure and temperature on the system efficiency of the BC were investigated. It was observed that with the increase of both parameters, the efficiency of the BC decreases slightly (Figure 8). This is due to the reduction of pressure difference between high and low side of the system. Additionally, with the increase of temperature the specific volume of the gas also increases, resulting in more energy consumption of compressor. Additionally, with the variation of compressor inlet temperature from 32 to 35 °C, the efficiency increases a bit and then decreases.

For the performance analyses of transcritical ORC system, turbine inlet pressure and temperature values were varied to determine the trend of energy efficiency. As seen from Figure 9, with the increase of pressure and temperature at the inlet of ORC turbine, the energy efficiency rate increases. The increase of the efficiency is from 1.9 % to 7.2 % while the pressure rates are varied between 7500 and 12300 kPa. But above the pressure rates of 12300 kPa, the efficiency tends to drop down slightly. However the effect of temperature on ORC efficiency is less than the effect of pressure. From Figure 9, it can be seen that the increase of efficiency is in a very narrow band with the temperature.

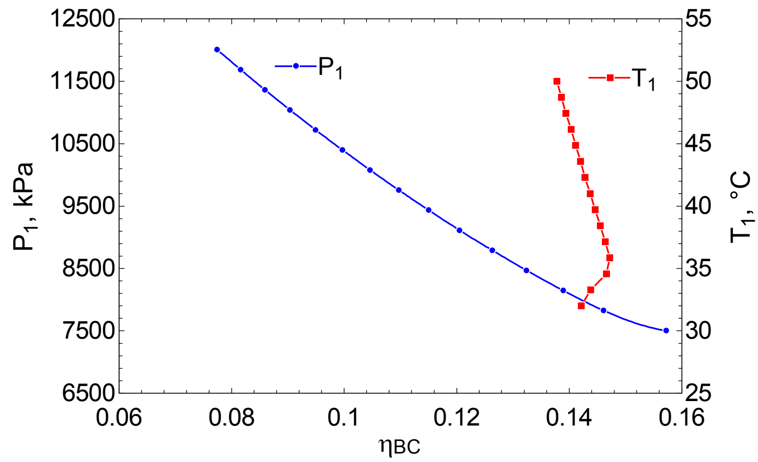

Fig. 8 Variation of energy efficiency with compressor inlet pressure temperature of BC

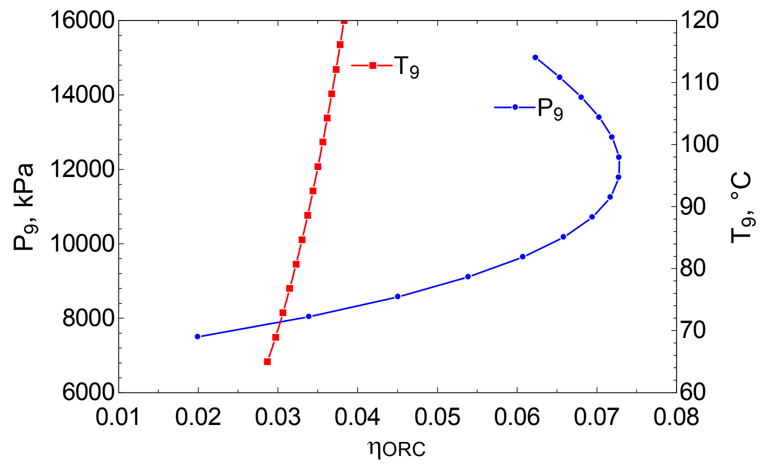

Fig. 9 Variation of energy efficiency with turbine inlet pressure and temperature of ORC

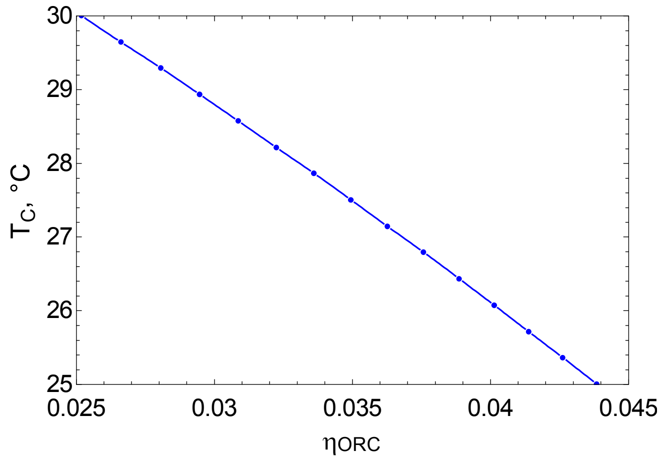

Fig. 10 Variation of energy efficiency with condenser temperature of ORC

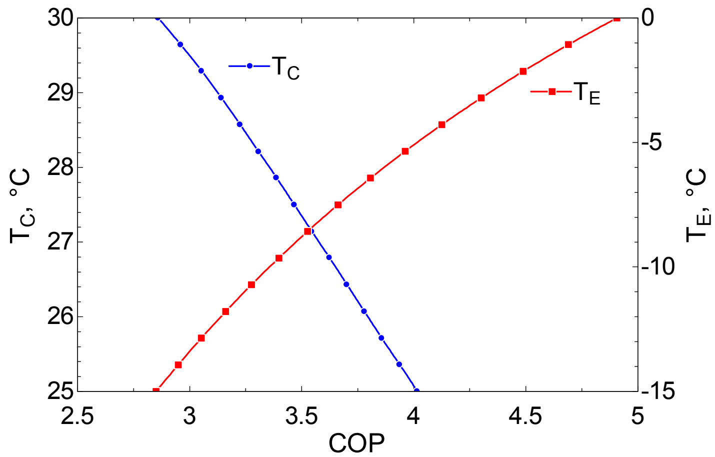

Fig. 11 Variation of energy efficiency with condenser and evaporator temperature of VCRC

In Figure 10 the variation of condenser temperature with the energy efficiency is shown for ORC. As declared previously, the condenser of the ORC is identical with the VCRC. Moreover, the upper temperature is limited to 30 °C since the critical temperature of CO_2 is 30.98 °C. As seen from the figure, the increase of condenser temperature has a negative effect on ORC efficiency.

For the VCRC system, the effects of condenser and evaporator temperatures on system efficiency, namely COP are given in Figure 11. The increase of condenser temperature results in a decrease of COP while with the increase of evaporator temperature, it increases. These variations are typical with that of simple refrigeration cycles and this can be explained in more detail with Carnot efficiency concept.

5. CONCLUSIONS

Design and modelling analysis of a solar driven combined power-refrigeration system using CO_2 was investigated comparatively. The system was consisted of supercritical BC, transcritical ORC and subcritical VCRC. The solar energy system was coupled with PTSCs which enabled temperature ranges of up to 400 °C. For the design parameters of the cycles, the net power generation of the BC was 865 kW, 120 kW for the ORC and the evaporation capacity of VCRC was 402.8 kW. From the analyses, the energy efficiency of the BC was found to be 12.9 %, the energy efficiency of the ORC was found to be 4.47 % and the COP value of refrigeration system was calculated to be 3.35. For the reported system parameters, the required total PTSCs aperture area was determined as 9801 m^2 which corresponded to PTSCs length of 2020.78 m. Additionally, the effects of solar radiation intensity, turbine inlet pressures and temperatures, condenser and evaporator temperatures were analyzed using CO_2 as a sustainable working fluid. This study points out that solar driven power-refrigeration system are compatible with other power generation systems and more detailed experimental studies should be carried out for green energy production using solar energy. Also, for supporting the Turkey's energy generation capacity, these kinds of systems can be a good alternative with solar energy. Besides, more attention should be given to modelling, analyzing, developing and installing of solar driven power generation systems.

REFERENCES

Al-Sulaiman F.A. (2013), "Energy and sizing analyses of parabolic trough solar collector integrated with steam and binary vapor cycles", *Energy,* **58,** 561-570.

Al-Sulaiman F.A. (2014), "Exergy analysis of parabolic trough solar collectors integrated with combined steam and organic Rankine cycles", *Energy Conversion and Management,* **77,** 441–449.

Aras, A., Balli, O. and Hepbasli, A. (2006), "Estimating the horizontal diffuse solar radiation over the central Anatolia Region of Turkey, *Energy Conversion and Management*, **47**, 2240–2249.

Atilgan, B. and Azapagic, A. (2014), "Life cycle environmental impacts of electricity from fossil fuels in Turkey", *Journal of Cleaner Production*, Available Online, In Press.

Cengel, Y.A., Boles, M.A. (2006). *Thermodynamics: an engineering approach*, 5th ed., McGraw-Hill, New York, USA.

Duffie, J.A. and Beckman, W.A. (2013), *Solar Engineering of Thermal Processes*, John Wiley & Sons Inc., New Jersey, USA.

EIE (2014), *Solar energy potential atlas of Turkey*, General Directorate of Renewable Energy, http://www.eie.gov.tr/, accessed on 10.12.2014, (In Turkish).

Energy (2011), *Blue Book*, Republic of Turkey Ministry of Energy and Natural Resources . http://www.enerji.gov.tr/File/?path=ROOT%2f1%2fDocuments%2fMavi+Kitap%2fMavi_Kitap_2011.pdf, accessed on 20.01.2015, (In Turkish).

Energy (2012), *Blue Book*, Republic of Turkey Ministry of Energy and Natural Resources, http://www.enerji.gov.tr/File/?path=ROOT%2f1%2fDocuments%2fMavi+Kitap%2fMavi_Kitap_2012.pdf, accessed on 20.01.2015, (In Turkish).

F-Chart (2015), *EES, F-Chart Software*. Engineering Equation Solver, http://www.fchart.com/, accessed on 10.12.2014.

Garg, P., Kumar, P. and Srinivasan K. (2013), "Supercritical carbon dioxide Brayton cycle for concentrated solar power", *The Journal of Supercritical Fluids,* **76,** 54–60.

Garg, P., Srinivasan, K., Dutta, P. and Kumar, P. (2014), "Comparison of CO2 and steam in transcritical Rankine cycles for concentrated solar power", *Energy Procedia,* **49**, 1138-1146.

Garg, P., Kumar, P. and Srinivasan K. (2015), "A trade-off between maxima in efficiency and specific work output of super- and trans-critical CO2 Brayton cycles", *The Journal of Supercritical Fluids,* **98**, 119-126.

Cheng, Z.D., He, Y.L, Cui, F.Q., Xu, R.J. and Tao, Y.B. (2012), "Numerical simulation of a parabolic trough solar collector with nonuniform solar flux conditions by coupling FVM and MCRT method", *Solar Energy,* **86,** 1770–1784.

Gunes, M. (2001), "Analysis of daily total horizontal solar radiation measurements in Turkey, *Energy Sources*, **23**, 563–570.

Iverson, B.D., Conboy, T.M., Pasch J.J. and Kruizenga A.M. (2013), "Supercritical CO2 Brayton cycles for solar-thermal energy", *Applied Energy,* **111,** 957-970.

Kalogirou, S.A. (2009). *Solar energy engineering: processes and systems*, 1st ed., Academic Press, Oxford, UK.

Kaygusuz, K. (2011), "Prospect of concentrating solar power in Turkey: The sustainable future", *Renewable and Sustainable Energy Reviews*, **15**, 808–814.

Koca, A., Oztop, H.F., Varol, Y. and Koca, G.O. (2011), "Estimation of solar radiation using artificial neural networks with different input parameters for Mediterranean region of Anatolia in Turkey", *Expert Systems with Applications*, **38**, 8756–8762.

Kumar K.R. and Reddy K.S. (2009). "Thermal analysis of solar parabolic trough with porous disc receiver", *Applied Energy,* **86,** 1804–1812.

Reddy, K.S., Kumar K.R. and Ajay, C.S. (2015), "Experimental investigation of porous disc enhanced receiver for solar parabolic trough collector", *Renewable Energy,* **77,** 308-319.

Reprisk (2015). *Special Report on MINT Countries: ESG Issues in Mexico, Indonesia, Nigeria and Turkey*. http://www.reprisk.com/reprisk-releases-special-report-on-mint-countries-mexico-indonesia-nigeria-and-turkey/, accessed on 19.02.2015.

Senol, R. (2012), "An analysis of solar energy and irrigation systems in Turkey", *Energy Policy*, **47**, 478–486.

Singh, R., Kearney, M.P. and Manzie, C. (2013), "Extremum-seeking control of a supercritical carbon-dioxide closed Brayton cycle in a direct-heated solar thermal power plant", *Energy*, **60**, 380-387.

Therminol (2014), *Therminol VP-1*, Heat transfer fluids by Eastman, http://www.therminol.com/products/Therminol-VP1, accessed on 10.12.2014.

Tiwari, G.N. (2003), *Solar Energy: Fundamentals, Design, Modelling and Applications*, Alpha Science International Ltd., Pangbourne UK.

Ulgen, K. and Hepbasli, A. (2004), "Solar radiation models Part 1: A review, *Energy Sources*, **26**, 507–520.

Vogel, T., Oeljeklaus, G., Görner, K., Dersch, J. and Polklas, T. (2014), "Hybridization of parabolic trough power plants with natural gas", *Energy Procedia,* **49,** 1238 – 1247.